Condensation Activation and Nucleation on Heterogeneous Aerosol Nanoparticles

V. Y. Smorodin[†,‡] and P. K. Hopke*[,†]

Department of Chemical Engineering, Clarkson University, Box 5708, Potsdam, New York 13699-5708, and Chemistry Department, Moscow State University, Moscow 119899, Russia

Received: December 7, 2003; In Final Form: April 17, 2004

Measurements of heterogeneous nucleation of several different compounds on different composition nuclei have shown several distinct patterns of nucleation and growth. Some of the specific behaviors for condensation activation of heterophilic (energetically nonuniform) aerosol nanoparticles have been theoretically analyzed based on a model of double-barrier nucleation (DBN) with an emphasis on scale and supersaturation effects. A new "semiempirical" method for collecting nucleation data from the condensation size spectrum of CN was developed. These results have been used to provide a qualitative interpretation of experimental data on the transformation of the initial size distribution spectrum of nanoparticles in a turbulent mixing condensation nuclei counter.

Introduction

The "activation" of condensation nuclei (CN) and cloud condensation nuclei (CCN) at some supersaturation depends on the aerosol particle size and its surface properties. Interest in the study of CN/CCN activation mechanisms has increased during recent years because of their large influence on the atmospheric environment and global climate change, as well as from the development of greatly improved experimental techniques.[1] Also, in recent time more attention has been paid to smaller aerosol sizes because of the understanding that the sub-micrometer aerosol fraction in the urban atmosphere has greater effects on human health.[2] Since the surface properties of such particles also determine the efficacy of their penetration and/or adhesion in human respiratory tracts, as well as their interactions with biomembranes, and their coagulation rates, there is a need for comprehensive research on the interfacial properties of such particles.

Recently, Mavliev et al.[3,4] developed a new method to improve a condensation nuclei counter (CNC) to measure the condensation of liquid compounds onto fine particles of various kinds. This research was oriented toward examining the relationship between the molecular properties of the working fluid and the particles. Mavliev et al.[4] have examined the nucleation of dibutyl phthalate, dodecane, dodecanol, and dodecanoic acid on NaCl, KCl, Ag, and AgCl particles. Lee et al.[5] have presented the results of a parallel study of the nucleation of the same working fluids on ultrafine carbon particles.

Many of the observations of CN behavior that could not be well understood by current heterogeneous condensation theories can be explained by taking into account the effects of the particle surface heterophilicity (energetic heterogeneity). The general term "heterogeneity" will be taken to mean both topographic and energetic heterogeneities on the particle surface. It should be noted that only polar liquids whose molecules have polar groups or permanent dipole moments demonstrate such effects, interacting differently with "active" and "passive" centers on the surface, while nonpolar liquids are indifferent to the surface heterophilicity. Our work will focus on the heterophilicity effects.

This idea which has been adopted as a working hypothesis will be examined where we will qualitatively interpret the unusual transformation of the particle size spectra observed in the experiments of Mavliev et al.[4] Taking into account the surface heterophilicity will result in new physical effects in condensational nucleation. As such, it will be necessary to make a change in the basic concepts of nucleation that leads to the explanation of referenced experiments.

Theoretical Background

Models of Condensation Nucleation on Aerosols. Figures 1 and 2 present schematic representations of a number of models of heterogeneous nucleation.[6−15] As known, the first theory of condensation on completely soluble particles was proposed by Köhler.[6] Insoluble condensation nuclei (CN) were analyzed by Krastanov[11] who regarded water nucleation on the particles of sizes smaller than the critical nucleus (when a liquid nucleus completely covers the particle, even at values of its wetting parameter, $m = \cos\theta < 1$, where θ is the contact angle). He derived an expression for Gibbs' energy of heterogeneous condensation nucleation:

$$\Delta G^*_{het} = \Delta G^*_{hom}(1 - 3x^2\cos\theta + 2x^3) \qquad (1)$$

where

$$\Delta G^*_{hom} = \frac{4\pi\sigma_{lv}R^{*2}}{3}, \quad x = \frac{R_0}{R^*}$$

ΔG^*_{hom} is the energy of homogeneous nucleation (no particles), σ_{lv} is the surface tension of the condensing liquid, R_0 is the particle radius, and R^* is the critical embryo radius, corresponding to the maximum of ΔG^*_{het}. An analysis of this expression shows that the particle is inactive if $\theta > 90°$. If $\theta < 48° 12'$ (corresponding to the inequality $x < 1$), the particle is always active, independent of the value of supersaturation, $S = \ln(p/$

* To whom correspondences should be addressed. E-mail: hopkepk@clarkson.edu. Fax: 315 268 4410.
† Clarkson University.
‡ Moscow State University.

10.1021/jp037742+ CCC: $27.50 © 2004 American Chemical Society
Published on Web 06/02/2004

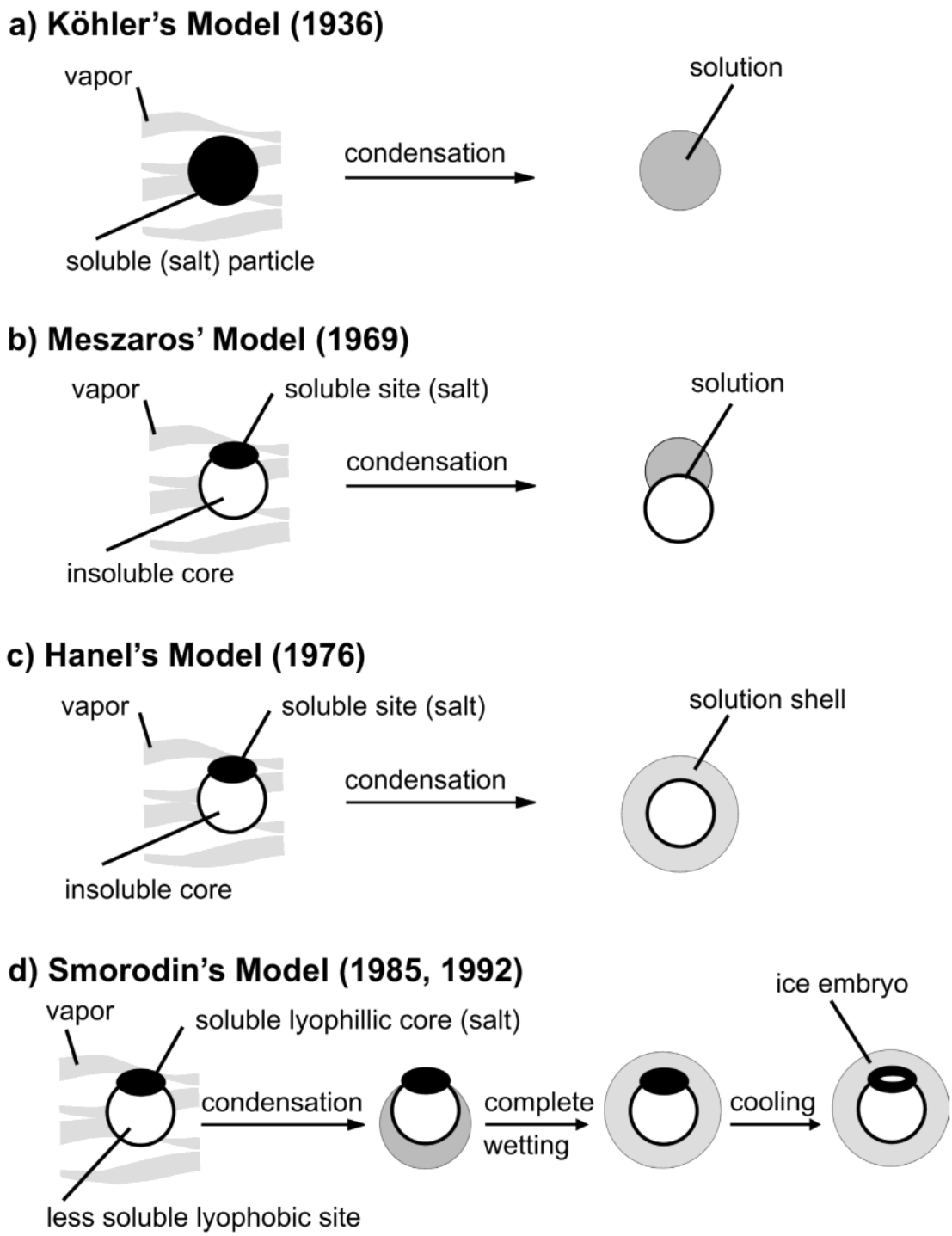

Figure 1. Schematic diagrams of models for heterogeneous nucleation on soluble particles.

p_s), where p_s is the saturation vapor pressure at temperature T and p is the partial pressure of the vapor.

Fletcher[12] investigated heterogeneous nucleation on homophilic aerosol particles for cases when an embryo has finite contact angles ($\theta > 0°$) and is smaller than the particle ($x > 1$). According to Fletcher, heterogeneous nucleation on an aerosol particle starts from an embryo liquid lens.

The standard scheme for calculating the heterogeneous condensation nucleation free energy used by Fletcher is based on the minimization of ΔG_{het} with respect to the "embryo" radius, R. Taking the grand potential as the characteristic thermodynamic function and limiting the parts of the one-component system with equi-molecular dividing surfaces, an equation can be written for the variable part of the potential (Gibbs' energy),

$$\Delta G_{het} = \sum_{ij} \sigma_{ij} S_{ij} + V \Delta G_v \qquad (2)$$

where

$$\Delta G_v = -\frac{R_v T \rho_l}{M_l} \ln S$$

is the "driving force" of condensation; $S = p/p_s$ is the vapor saturation; V is the droplet volume; R_v is the universal gas

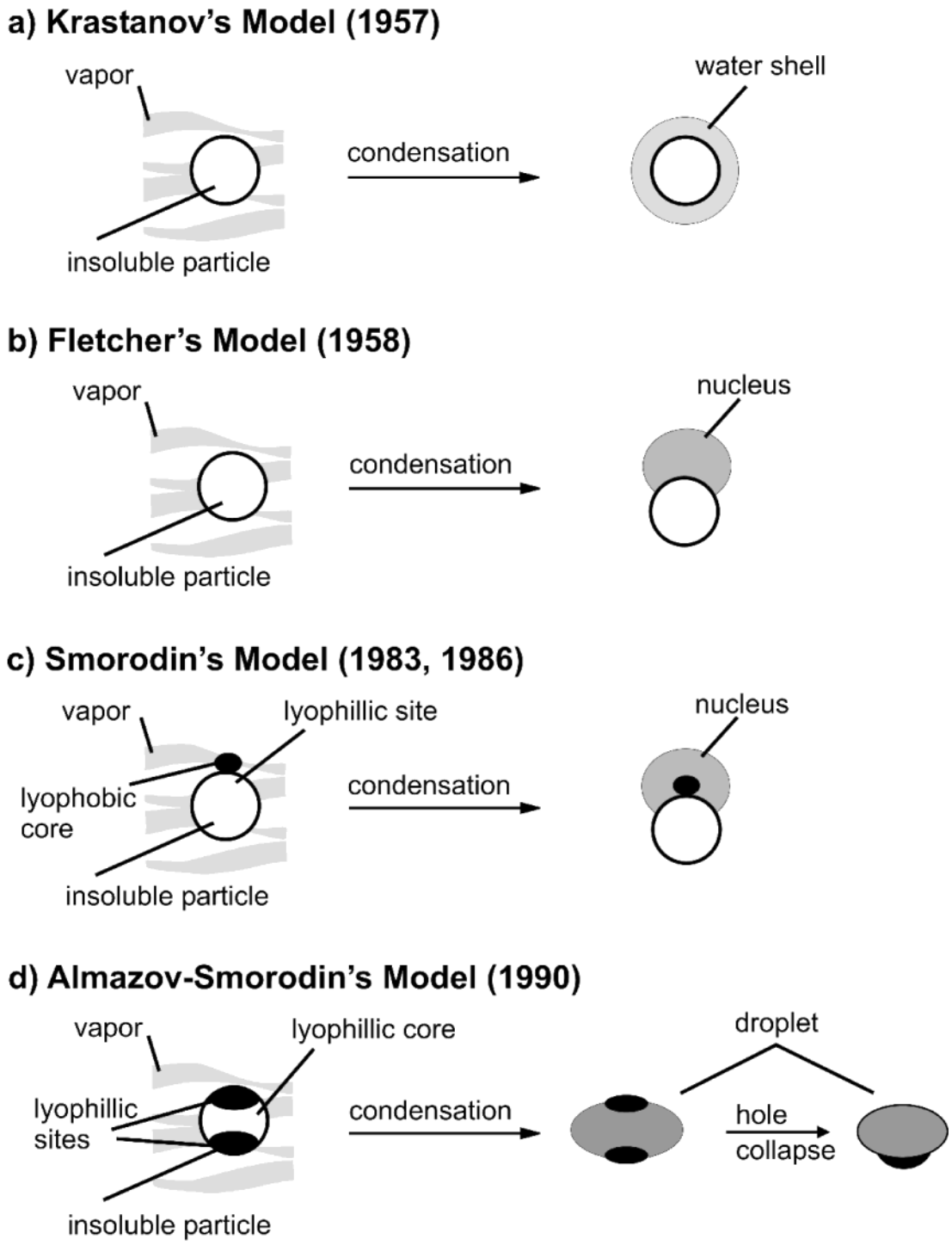

Figure 2. Schematic diagrams of models for heterogeneous nucleation on insoluble particles.

constant; M_l is the molar weight of liquid; σ_{lv} is the surface tension of liquid; and ρ_l is its density. The energy of embryo formation can be identified as the maximum in the curve ΔG_{het} vs R; setting $\partial(\Delta G_{het})/\partial R$ at $R = R^*$ for fixed $m = \cos\theta$ permits the calculation of the Kelvin's radius of embryo given by

$$R^* = -\frac{2\sigma_{lv}}{\Delta G_v} = \frac{2M_l\sigma_{lv}}{R_v T\rho_l \ln S} \tag{3}$$

The energy of heterogeneous nucleation at a homogeneous aerosol particle, in frameworks of classical thermodynamics, can be presented by Fletcher's formula:[12]

$$\Delta G^*_{het} = \Delta G^*_{hom} f(m,x) \tag{4}$$

$$f(m,x) = \frac{1}{2}\left\{1 + \left(\frac{1-mx}{h}\right)^3 + x\left[2 - 3\left(\frac{x-m}{h}\right) + \left(\frac{x-m}{h}\right)^3\right] + 3mx^2\left(\frac{x-m}{h} - 1\right)\right\} \tag{5}$$

$$\Delta G^*_{hom} = \frac{16\pi M^2\sigma^3}{3(R_v T\rho \ln S)^2}, \quad x = R/R^*, \quad h = \sqrt{1 + x^2 - 2mx} \tag{6}$$

Mahata and Alofs[16] modified Fletcher's theory to consider nucleation on an insoluble, partially wettable, spherically

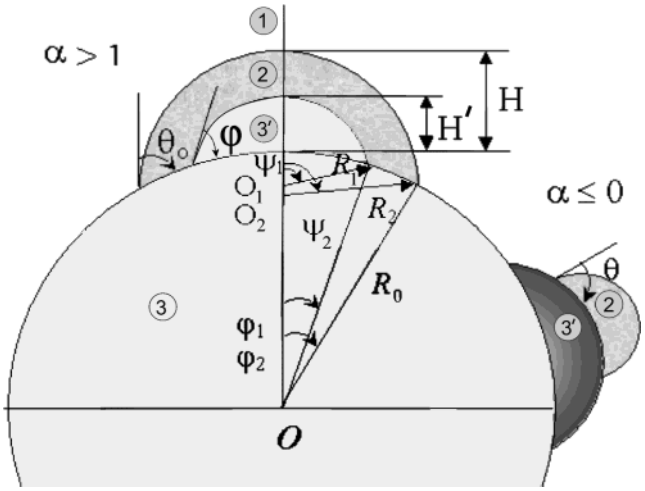

Figure 3. Model of heterogeneous nucleation on a heterophilic particle.

concave substrate; the only change from the previous theory was one of geometry. The concavity or roughness of the particle surface significantly enhanced the condensation activity of aerosol particles. Studying atmospheric CN, Meszaros[7] proposed a model of the aerosol particle containing an insoluble core and a soluble part in the form of a lens. Heterogeneous condensation nucleation of binary systems was examined, in part, by Hamill et al.[17] Many authors have analyzed condensation activation of CN based on simplified spherical symmetric models of particles covered with liquid shells (e.g., Malm[18]).

In prior studies by Smorodin and co-worker,[13,14,19,20] a general model of insoluble mixed aerosol particles (MAP) with "active sites" (AS) was proposed. Figure 3 provides the schematic view of this model that represents the principal features of real conglomerates of mixed composition, for example, formed by combustion, condensation, and coagulation of the components in the atmosphere. It is assumed that on the surface of the insoluble particle of radius R_0 (3), there are nonoverlapping zones of different character. Among these zones, there are insoluble, active nucleation sites with radii of curvature R_1, "edge" angle ϕ_0, a surface concentration (of active centers), n, a coefficient of wetting of active site with new phase (an embryo: (2)) $m_l = \cos \phi_1$, and a coefficient of wetting of the main (inactive) particle with the embryo, $m_o = \cos \phi_2$. It is assumed that the spherical embryo of stable phase (2), with radius R_2, nucleates from the supersaturated vapor phase (1) onto the surface of the particle, simultaneously covering $N > 0$ active "centers".

In Figure 3, the case of $\alpha > 1$ corresponds to a situation when the embryo is larger than the active site and overlaps the last one, while $\alpha \leq 1$ corresponds to a situation when an embryo is smaller than the active center. A detailed discussion of this basic model and exact criteria of the different surface activity of the MAPs have been presented by Smorodin and co-worker.[13,14,19,20]

It has been found in both of these cases that the energy of heterogeneous nucleation can be presented in a standard form where Fletcher's "geometrical factor" $f(m,x)$ must be replaced with a more general "heterogeneity factor" F.[13−15,20] Later, this approach was refined by proposing a model of MAP when both the partial core and AS are soluble with different solubility rates.[10,21]

Some models of insoluble aerosol particles with a heterophilic surface have been reviewed in refs 22−25, where relationships between processes of adsorption, wetting, and condensation activation were analyzed. It was concluded that the thermodynamic evolution of the liquid phase on the heterophilic particle is related to overcoming the additional extrema of its free energy, compared to the case of the homophilic particle. These energetic barriers affect the processes of vapor adsorption and heterogeneous condensation. A series of new physical effects has been theoretically predicted, for example, "quasi-cavitation condensation", "double barrier nucleation", and atmospheric humidity hysteresis-dependent light scattering coefficient.

An alternative hypothesis was proposed by Lazaridis et al.[26] in which they suggest that variation in surface roughness of the particle could have an influence on the contact angle and, thus, on the formation of the critical embryo on the surface. Thus, it may be that both variations in roughness ("concaves") and chemical "active sites" at surfaces can produce similar activation effects on the condensation nucleation. A rigorous theoretical analysis of the relative role of each effect must be based on more complete experimental knowledge of surface properties of aerosol particles than is currently possible and must be deferred to future studies.

Application to Heterogeneous Condensation Nucleation

The goal of this present study is to analyze the possible effects of surface heterophilicity of insoluble aerosol particles on the evolution of their mean size spectra during heterogeneous condensation previously measured experimentally by Mavliev et al.[3] The experimental system is shown schematically in Figure 4. The basic components are the particle generators, the condensation nuclei counters (CNC), and the differential mobility analyzer (DMA). The TM CNC was the same as that described previously.[3,4]

Experimental Results. To provide a perspective on the problem of understanding heterogeneous condensation nucleation, some of the results of Mavliev et al.[4] will be presented. Figure 5 shows the nucleation of octadecanoic acid on NaCl particles at a saturator temperature of 353 K and a saturator temperature of 293 K. The size distributions were measured for various partial pressures of the working fluid vapor that is achieved by varying the ratio of flows through the wet and dry sides of the saturator. It can be seen that as the pressure of the acid increases, the size distribution smoothly increases to larger sizes. In this case, all of the particles are bigger than their Kelvin diameters. Thus, they activate and subsequently grow. The dispersion of the distributions increases with increasing vapor concentration so it appears that the initially larger particles in the distribution grow more rapidly than the smaller particles.

Figure 6 presents the results of experiments for the heterogeneous nucleation of octadecanol on silver particles[4] for a saturator temperature of 353 K and condensor temperature of 293 K. In this case, it can be observed that there are some nuclei on which nucleation and growth occurs and there is increased growth with increasing partial pressures of the octadecanol. It is this example that will be examined qualitatively in more detail.

Theoretical Approach

Model. Assuming that possibly to neglect with a coagulation process in the CNC, as it follows from experimental conditions and elementary estimations, the working hypothesis is that surface heterophilicity plays a major role in the unusual transformation that was detected in the condensation size spectrum.

Consider first one of the simplest and convenient models of the heterophilic aerosol particle: an insoluble spherical particle of radius R_0 and parameter $m = \cos \theta_0$ that contains an "active site" of radius R_d and $m_c = \cos \theta_c$. This model can be regarded

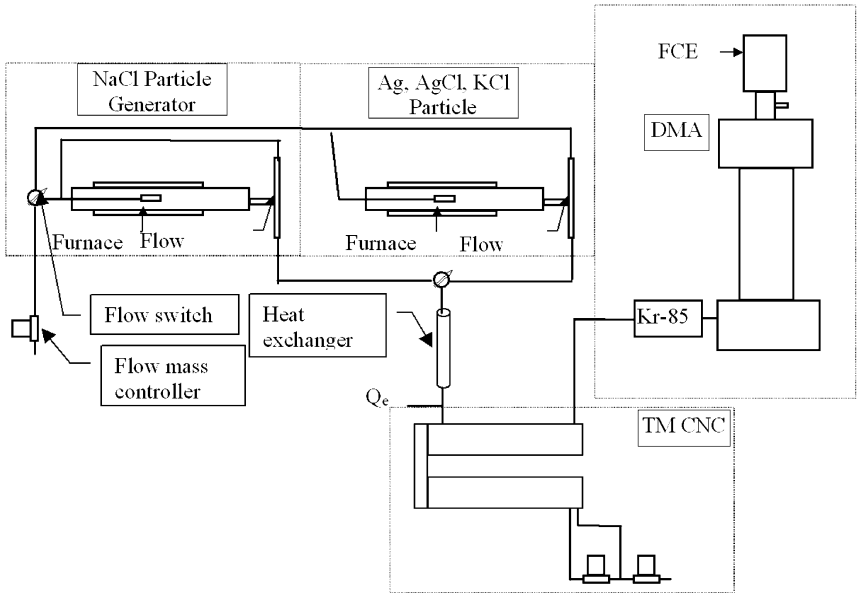

Figure 4. Schematic diagram of experimental system for heterogeneous nucleation measurements taken from Mavliev et al.[4]

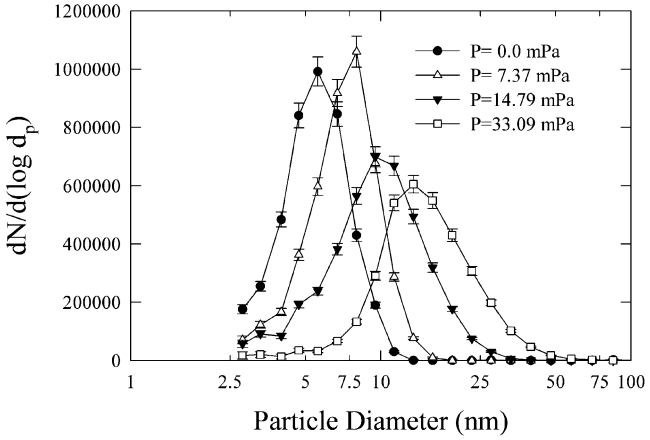

Figure 5. Size distribution of NaCl particles at various pressure of octadecanoic acid vapor as measured by Mavliev et al.[4]

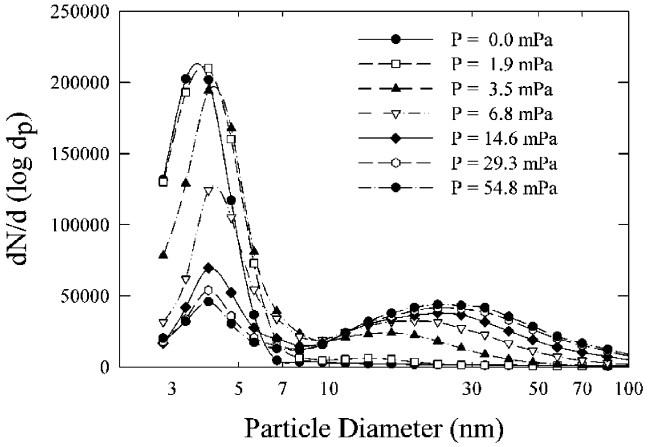

Figure 6. Size distribution for Ag particles at various pressures of octadecanol vapor as measured by Mavliev et al.[4]

as a simplified version of the model presented in Figure 3, where parameter $\varphi = 0$. Therefore, this model is similar to Fletcher's model of the particle with active sites.[12] However, another case will be considered in which during its evolution, the embryo can be both smaller and larger than the site. Analyzing the process of heterogeneous nucleation of liquid phase on this particle, classical Gibbs thermodynamics will be applied. The effects of linear tension on the droplet contact angle and its consequence on heterogeneous condensation was first suggested by Scherbakov.[27,28] It was then developed further by Scheludko and co-workers[29] and later by many others. The effect of the linear tension on nucleation in the framework of classical nucleation theory was examined by Lazaridis.[30] In the present study, the contribution of linear tension to the embryo perimeter will be neglected in order to focus only on the heterophilicity effects.

Double-Barrier Nucleation on a Spherical Heterophilic Particle. For this model, the classical scheme of Gibbs' energy minimization must be modified because of the appearance of additional extreme values in the free energy of the embryo. In other words, there are additional conditions affecting the stability of the liquid phase on a heterophilic surface.

Using variation techniques for the free energy functional to analyze the drop stability on a heterophilic particle,[23,25] the following expression can be written for the variation of the drop perimeter at the boundary of the "active site" (at $V, T = \text{const}$):

$$\delta(\Delta G_{\text{het}}) = \begin{cases} C(m_c - m)\delta\varphi, & \delta\varphi \le 0; \\ C(m - m_0)\delta\varphi, & \delta\varphi > 0; \end{cases} \tag{7}$$

where $C = \text{const}$; $\delta\varphi$ is the variation of the space angle near a value $\varphi = \varphi_d$, where φ_d is the space angle of the active site. From eq 7, it follows that ΔG_{het} has a minimum value at $\delta\varphi = 0$ (corresponding to the fixed perimeter of the drop) and the equilibrium contact angle varies as $\theta_c \le \theta \le \theta_0$; that is, a displacement of the drop perimeter in any direction leads to an increase in ΔG_{het}. This dependence of the contact angle on the drop (film) volume on the heterophilic surface has been first observed experimentally[22] and then thoroughly studied theoretically.[15,23,25,31]

This peculiarity of the wetting of the heterophilic surface leads to changing the standard techniques of estimating the nucleation free energy. Obviously, for a fixed perimeter, the drop volume can increase if the contact angle θ increases and the radius of curvature, R, decreases. When $\theta = \theta_0$, the minimum (and the barrier preventing the displacement of the drop perimeter) disappears and the drop grows freely throughout the particle "matrix" with a constant contact angle θ_0. Thus, the radius of curvature of the drop on the aerosol particle with an "active

site" depends nonmonotonically on its volume: first for $\varphi < \varphi_d$, $\theta = \theta_c$ (Region I) and R increases as V increases to some critical value $V = V_{2,min}$ with a maximum value of $R = R_{2,max}$; for $\varphi = \varphi_d$, $\theta_c < \theta < \theta_0$ (Region II) it decreases to $R = R_{2,min}$; and for $\varphi > \varphi_d$, $\theta = \theta_0$. As in the case of the "double-barrier nucleation" presented earlier as a model for a flat heterophilic surface,[25] the dependence of the Gibbs free energy on the drop volume can have two maximums. A second maximum, which can be either higher or lower than the first ("classical") one, corresponds to overcoming an energetic barrier at the heterophilic surface.

Formalizing this approach, the expression for the Gibbs free energy of the drop on the heterophilic particle is written in a dimensionless form in order to be more convenient for the next step in the analysis:

$$\Delta\Gamma = \frac{\Delta G_{het}}{2\pi R_0^{\,2}\sigma_{lv}} = \begin{cases} [\chi^2(1-\cos\psi_1) - m_c(1-\cos\varphi_1)] - \lambda\omega_1(\chi,m_c), & \omega_1 < \omega_{01}; \\ [\chi^2(1-\cos\psi_2) - m_c(1-\xi)] - \lambda\omega_2(\chi,m(\chi)), & \omega_{01} \le \omega_2 \le \omega_{02}; \\ [\chi^2(1-\cos\psi_3) - m_c(1-\xi) - m_0(\xi-\cos\varphi_3)] - \lambda\omega_3(\chi,m_0), & \omega_{01} < \omega_3; \end{cases} \tag{8}$$

$$\omega = \frac{3V}{\pi R_0^{\,3}} = \begin{cases} \omega_1 = \chi^3(2 - 3\cos\psi_1 + \cos^3\psi_1) - (2 - 3\cos\varphi_1 + \cos^3\varphi_1), & \omega_1 < \omega_{01}, & I; \\ \omega_2 = \chi^3(2 - 3\cos\psi_2 + \cos^3\psi_2) - (2 - 3\xi + \xi^3), & \omega_{01} \le \omega_2 \le \omega_{02}, & II; \\ \omega_3 = \chi^3(2 - 3\cos\psi_3 + \cos^3\psi_3) - (2 - 3\cos\varphi_3 + \cos^3\varphi_3), & \omega_{02} < \omega_3, & III; \end{cases} \tag{9}$$

where

$$\cos\varphi_i = \frac{1 - m_i\chi}{d_i}, \quad \cos\psi_i = \frac{m_i - \chi}{d_i}, \quad d_i = \sqrt{1 + \chi^2 - 2m_i\chi},\ i = 1,2,3$$

$$m_i = \begin{cases} m_c \le m_0, & I, & i = 1; \\ m = \cos\theta, & \theta \le \theta \le \theta, & II, \quad i = 2; \\ m_0, & III, & i = 3; \end{cases}$$

For simplicity, we regard the case when $0 \le m_0 \le m_c \le 1$, where

$$\chi = R/R_0, \quad \lambda = \frac{R_v T \rho_l R_0 \ln(p/p_S)}{6M_l\sigma_{lv}} = \lambda_0/\xi, \quad \xi = R_d/R_0$$

The relationship between θ and χ in region II follows from

$$\varphi = \xi \text{ or } 1 - m\chi = \xi\sqrt{1 + \chi^2 - 2m\chi} \tag{10}$$

where it follows

$$\chi(\theta) = \frac{(1-\xi^2)\cos\theta \pm \xi\sqrt{1-\xi^2}\sin\theta}{\cos^2\theta - \xi^2} \tag{11}$$

For angles $\theta \le 90°$, the negative solution should be taken as follows from asymptotic analysis. Then from eq 11, it follows

$$\chi_{2,min} = \frac{(1-\xi^2)\cos\theta_0 \pm \xi\sqrt{1-\xi^2}\sin\theta_0}{\cos^2\theta_0 - \xi^2} \tag{12}$$

$$\chi_{2,max} = \frac{(1-\xi^2)\cos\theta_c \pm \xi\sqrt{1-\xi^2}\sin\theta_c}{\cos^2\theta_c - \xi^2} \tag{13}$$

With use of eqs 9 and 10, the values for $\omega_{01} = \omega_1(\chi_{2,max}, m_c)$ and $\omega_{02} = \omega_3(\chi_{2,min}, m_0)$ can be estimated. The calculated dependencies, $\chi = \chi(\omega)$, are presented in Figure 7. With analysis of these plots for cases of the nonmonotonic behavior of $\chi = \chi(\omega)$, and after the dimensionless Kelvin's radius ($\chi_K = R^*/R_0 = -2\sigma_{lv}/(R_0\Delta G_V)$) has been chosen as a "natural scale", three situations can be identified during heterogeneous nucleation:

$$\begin{aligned} &\text{(a) } \chi_K \ge \chi_{2,max} \text{ (low supersaturation)} \\ &\text{(b) } \chi_{2,min} < \chi_K < \chi_{2,max} \text{ (medium supersaturation)} \\ &\text{(c) } \chi_K \le \chi_{2,max} \text{ (high supersaturation)} \end{aligned} \tag{14}$$

These regions are shown in Figure 7 with the vertical dotted lines. In case (a), the "critical embryo" overlaps the "active site", and its thermodynamic evolution and the nucleation rate are determined only by the particle "matrix" (outside of the "site"); a radius of the liquid phase grows monotonically when its volume increases.

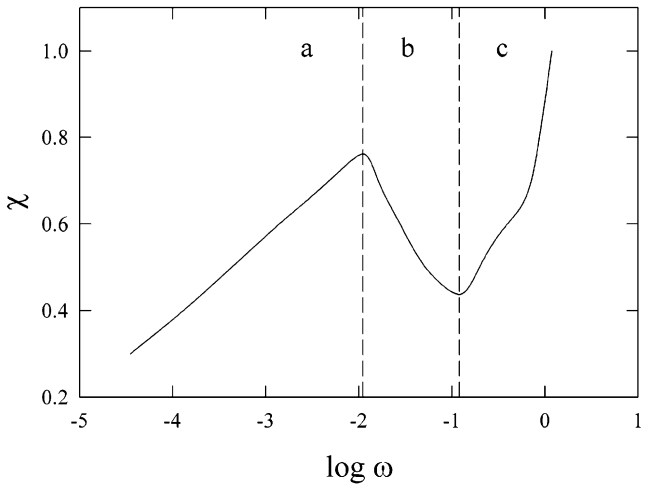

Figure 7. Dependence of the drop radius, χ, on its volume, ω (dimensionless variables).

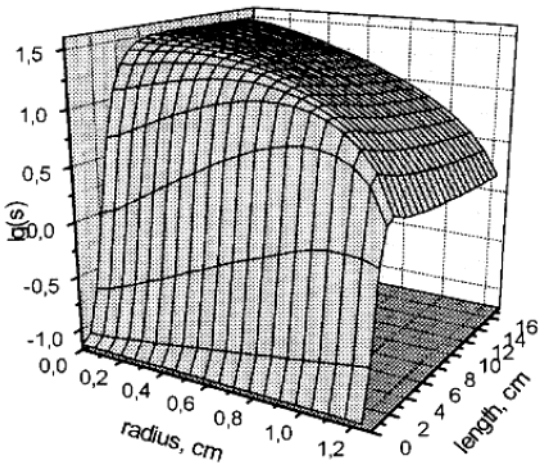

Figure 8. Typical dependence of vapor saturation in the condensor on the radius and a length parameter for octadecanoic acid at $T = 293$ K (calculations).

In case (b), after the initial nucleation at the "active site," the radius of the "super-critical" embryo grows until it reaches a maximum value. It then decreases to a value smaller than the initial Gibbs' radius. This behavior means that the nucleation stops if $S^* = \text{const}$, and the second maximum of the Gibbs energy as a function of the embryo volume is higher than the first classical energy maximum. To overcome the second barrier, the supersaturation would need to be increased in the system (or be able to do additional work).

In case (c), when the initial supersaturation is relatively high, once started, nucleation will develop without stopping, overcoming the second barrier (maximum) that is lower than the classical Gibbs' nucleation maximum.

With use of eqs 12 and 13, a quantitative criterion for case (b) can be developed as follows:

$$\frac{\cos\theta_0(1-\xi^2)-\xi\sqrt{1-\xi^2}\sin\theta_0}{\cos^2\theta_0-\xi^2} < \frac{2\sigma_{lv}M_l}{R_vT\rho_lR_0\ln S} < \frac{\cos\theta_c(1-\xi^2)-\xi\sqrt{1-\xi^2}\sin\theta_c}{\cos^2\theta_c-\xi^2} \quad (15)$$

New Definition of Heterogeneous Nucleation Free Energy on Heterophilic Particles. A detailed study of the dependence of the Gibbs free energy of the nucleating phase as a function of its volume, $\Delta G_{het} = f(\omega)$, permits the development of criteria for distinguishing between one- versus two-barrier nucleation, and estimating the values of the nucleation barriers requires an analysis of ΔG_{het} at its extremes. This energy is presented in terms of elementary functions in eq 2, but such an analysis is too complicated for this current work and will be developed more fully in the future. Thus, this presentation will only present a qualitative view of the nucleation and growth processes. The information on the nature of the particle surfaces and other critical data are not yet available to permit a quantitative estimation of this new nucleation model. However, the important differences in the model of nucleation on a heterophilic particle can be described and results qualitatively compared to classical nucleation theories. The differences are (1) changes of contact angle during the embryo growth and (2) nonmonotonic dependence of the embryo radius on its volume. From these differences, it follows that an analysis of the heterogeneous nucleation free energy at the extreme values of drop radius cannot be done (as was recognized by Gibbs and Fletcher). Instead of the radius, the drop volume should be used as the parameter, taking into account a relationship between χ and θ in the 2-region. In other words, the minimization of the energy of heterogeneous nucleation, instead of a partial derivation, $\partial(\Delta G_{het})/\partial R$, (by an embryo radius) should involve the total derivation (by its volume as a variable):

$$\frac{d\Delta G_{het}}{d\omega} = \frac{\partial\Delta G_{het}}{\partial\omega} + \frac{\partial\Delta G_{het}}{\partial\chi}\left(\frac{\partial\omega}{\partial\chi}\right) \quad (16)$$

With use of this formula, eqs 8 and 9, and some rearrangements, it is found that, in the first or third regions, the maximum value of Gibbs' energy of heterogeneous nucleation can be calculated from Fletcher's theory using eq 2. The position of the maximum energy depends on the saturation (criteria (a) or (c) above). In the second region, if the criteria (b) or the criterion in eq 15 is satisfied, there could be two extreme values: one minimum and one maximum, or there could be only one minimum. After some manipulation, the energy of heterogeneous nucleation on the heterophilic aerosol particle is given by

$$\Delta G^*_{het} = \Delta G^*_{hom} F(m(x),x) \quad (17)$$

where $F(m(x),x)$ is the "heterophilic factor" that is a "stripe" function, in general, nonmonotonic. For homophilic, smooth particles, the "heterogeneous factor" $F(m(x),x)$ reduces to Fletcher's "geometric factor", $f(m,x)$. In the case of two maximums (ΔG^*_i, $i = 1, 2$), the energy of nucleation of the critical embryo for a fixed supersaturation, S, is defined as

$$\Delta G^*_{het} = \text{Max}\{\Delta G^*_1, \Delta G^*_2\} \quad (18)$$

Estimations. These new results on the double-barrier nucleation (DBN) phenomenon generate two reasonable questions: (1) "Does it correspond to any practically important situations?" and (2) "Does it depend on the particle radius at other fixed parameters?"

To answer these questions, the relevant numerical estimations of the temperature and supersaturation in the turbulent mixing aerosol chamber are analyzed. The T and S estimates have been made by Anisimov and are presented in Figure 8. In this experiment, octadecanoic acid ($C_{18}H_{34}O_2$) was used as the "working liquid" ($M_l = 283$ g/mol, $\rho_l = 0.8$ g/cm^3, $T = 293$ K) that was condensed on nanometer particles at typical super-

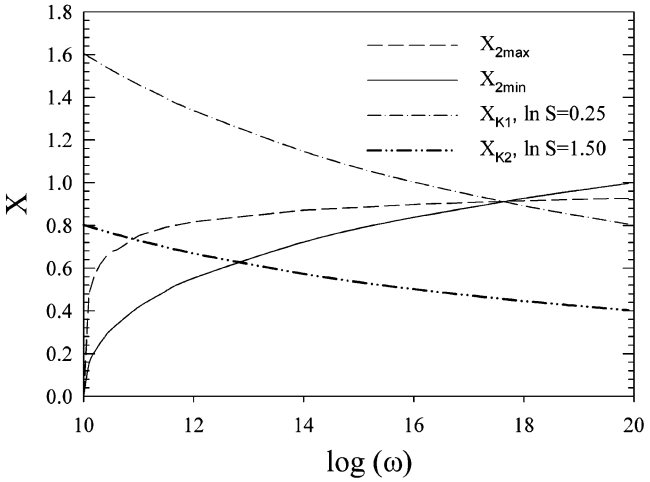

Figure 9. Dependencies of parameters $\chi_{2,\min}$, $\chi_{2,\max}$, and χ_K (at $\ln S = 0.25$ and $\ln S = 0.5$) on the particle radius (R_0, nm) at $R_d = 10$ nm, $\theta_0 = \pi/3$, and $\theta_c = \pi/20$.

saturations, S, of 2−4. Over the range of temperature of interest, a calculated value of $\sigma_l = 20$ dn/cm was used.

Plots in Figure 9 present the calculated values of the parameters χ_K, $\chi_{2,\min}$, and $\chi_{2,\max}$ at different values of S. For particles in the range of $R_0 = 5-30$ nm and $S = 1-4$, typical values of parameters are $\chi_{2,\min} \in (0.4, 0.8)$, $\chi_{2,\max} \in (0.8, 1.2)$, and $\chi_K \in (0.5, 0.8)$. For these calculations, values of $m_o = D/3$ and $m_c = D/20$ were used. These estimates show that case (b) with "double-barrier" nucleation has occurred in these experiments. From Figure 9, it can be seen that, at $\ln S = 0.25$, the χ_{K1} curve intersects the χ_{2Max} and χ_{2Min} curves so that there is no value at which the Kelvin radius satisfies the inequality in eq 15. However, the $\ln S = 1.5$ curve does have a length that satisfies eq 15. Thus, in the region between χ_{2Min} and χ_{2Max} with $\ln S > 0.25$, double-barrier nucleation (DBN) can occur and it follows from this plot that theoretically DBN may occur if $\ln S > 0.25$. Calculations such as those that were used to generate Figure 9 show that the criteria a, b, and c depend on particle size, particularly in the size range in 10−15 nm. The effect disappears for larger particles.

Summarizing these estimations, it can be concluded that the energy and rate of heterogeneous nucleation (condensation) of polar liquids on heterophilic aerosol particles at $S = \text{const}$ depends on the particles size. For smaller particles, the rate of nucleation is smaller since there are fewer active sites on the limited surface area with the potential of no available site and there needs to be an overlap of the "site" by the critical embryo. For larger particles, the nucleation rate is higher due to the greater role of "active sites." There can be more sites because of surface heterogeneity and easier nucleation since lower curvature is required to form the nucleus. However, in some cases, when the second barrier is higher than the first one, DBN can occur that stops the initial nucleation. Therefore, depending on the particle size and supersaturation, heterophilic particles can have different "activation" abilities. Heterogeneous nucleation on homophilic particles cannot have such properties because the plots of Fletcher's function, $f(m,x)$, show the effects of curvatures on the nucleation free energy for all relevant situations are relatively smooth.

New Method of Deriving Heterogeneous Nucleation Data on the Single Aerosol Particle from the Experimental Condensation Size Spectra Statistics. A relationship needs to be developed between the experimental data for condensation activation of CN and their nucleation properties. This relationship must link nucleation on a single particle with the macroscopic condensation data of the aerosol ensemble by examining nucleation theory and the condensation experiments. This methodology is only "semiempirical". For this purpose Carte's formula for the probability of nucleation of monodisperse nuclei[32] will be applied to our case of heterogeneous condensation nucleation,

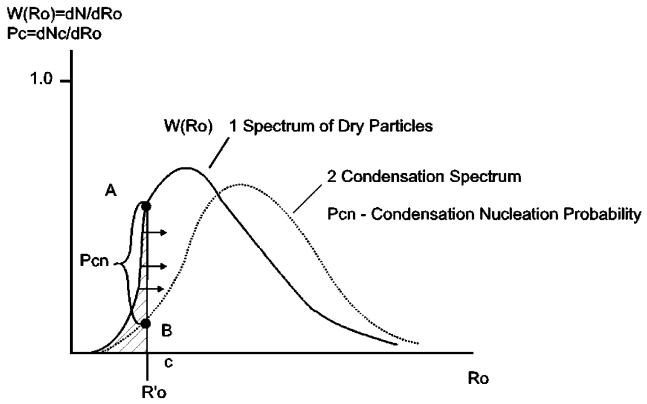

Figure 10. New "semiempirical" concept of calculating the nucleation data from the condensation spectrum.

$$P_c^0(R_0,t) = 1 - \exp(-J_c t) \tag{19}$$

where $P_c^0(R_0,t) = n_c(R_0,t)/n_0$ is the ratio of concentration of activated particles, $n_c(R_0,t)$, to initially dry particles, n_0, and J_c is the nucleation rate for nuclei of a particular size. Generalizing this formula for the polydisperse system includes the function of the particle size distribution, $W(R_0)$:

$$P_{cn}(R_0,t) = W(R_0)[1 - \exp(-J_c t)] \tag{20}$$

Thus, there is size dependence in both terms in this equation. Figure 10 provides a conceptual framework for discussing the conceptual framework of the approach. The number of particles at point B, $N(B)$, is the result of (1) outgoing number (to the right side) of nucleated particles at the point A, $N-$, and (2) incoming number of nucleated particles of smaller size (from the left side), $N+$. Thus, $N(B) = N(A) - N_- + N_+$. Obviously, if $N(B) \ll N(A)$, $N(B) \gg N(A) - N_-$, the section AB is approximately equal to the number of nucleated particles:

$$P_{cn}(R_0,t) \approx W(R_0)[1 - \exp(-J_c t)] \tag{21}$$

if $1 \gg \exp(-J_c t)$, or $J_c t > 1$.

Such situations occur for nanoparticles since the effect of their curvature strongly changes the rate of nucleation, J_c, with decreasing the particle radius, R_0. At point B′, satisfying the equation $1 = \exp(-J_c t)$, the fluxes of particles from the left and to the right are equal.

Usually, the residence time in the chamber is determined by the chamber geometry and is some constant, $t = t_0$. Thus, t is replaced by t_0. The characteristic time, t_0 , is defined as the time the particle resides within the zone in the CNC where nucleation can occur. For the CNC, it can be defined as the time between the single-particle input and output in the CNC module. This time was estimated in the CNC to be about 0.3 s (i.e., $t_0 \approx 0.3$ s).

Taking the logarithm of both sides of eq 21 and after rearrangement, the expression is written as

$$J_c = -\frac{1}{t_0}\ln[1 - P_{cn}/W(R_0)] \tag{22}$$

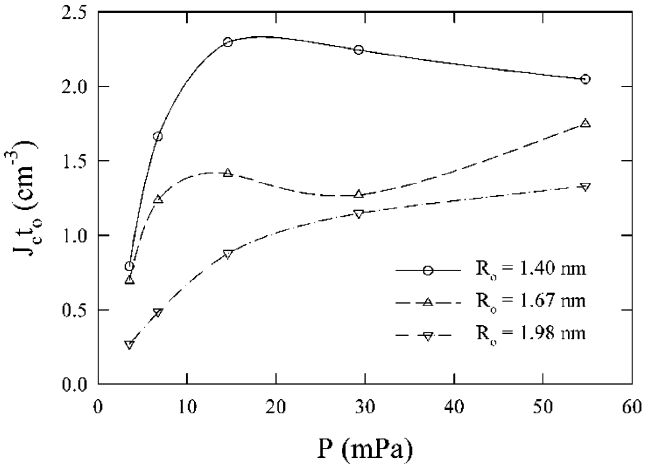

Figure 11. Dependence of the condensation nucleation, $J_c t_0$, on the vapor pressure for different values of the Ag-nanoparticle radii, R_0, calculated from the experimental condensation size spectrum.

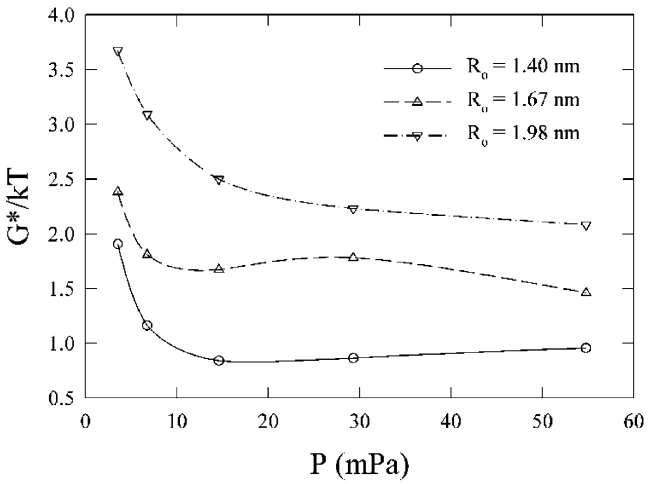

Figure 12. Dependencies of the condensation nucleation free energy ($\Delta G_{het}/kT$) on the vapor pressure for different values of the Ag-nanoparticle radii, R_0, calculated from the experimental condensation size spectrum.

The considerations presented above permit the collection of sufficient empirical information concerning the rate (and energy) of nucleation on the single particle from the condensation activation spectrum of CN (in its differential form) from its advancing branch. It should be noted that the structure of the theory has not been specified, but the use of the new "semi-empirical" method can be used to test different types of nucleation theories from classical or any of its modifications.

The next part of the interpretation of the experimental data depends on a specific form of the nucleation theory. In part, for classical nucleation theory, where the nucleation rate can be presented by,[12]

$$J_c = 4\pi R_0^2 K \exp\{-\Delta G^*_{het}/kT\} \quad (23)$$

it follows that

$$\Delta G^*_{het} = -kT \ln\left\{-\frac{1}{4\pi R_0^2 K t_0}\ln[1 - P_{cn}/W(R_0)]\right\} \quad (24)$$

where K is the pre-exponential factor. For alternative theories, the representation of the nucleation free energy is typically different.

Using these formulas (eqs 22 and 24), one can calculate the condensation−nucleation rate, $J_c = f(R_0)$, using the experimental data for $W(R_0)$ and P_{cn}. For homophilic particles, a monotonic dependence of J_c on the vapor pressure, P, or the particle radius, R_0, should be expected in accordance with classical nucleation theory. For the heterophilic particles, these dependencies must be nonmonotonic. Then, having found the empirical values of the nucleation rates, the condensation nucleation free energy, ΔG^*_{het}, can be evaluated using the formulas given above. Re-writing eq 24 as

$$\Delta G^*_{het}/kT = -\ln[J_c^{emp}(R_0,P)t_0/R_0^2] + \ln(4\pi K)$$
$$= -\ln[J_c^{emp}(R_0,P)t_0/R_0^2] + \text{const} \quad (25)$$

In this paper, the focus is on qualitatively estimating the effects of surface heterogeneity on the Gibbs nucleation free energy rather than its exact value. The value of the constant was initially set to zero and then a value was added to shift the plots shown in Figures 11 and 12 so that the abscissa values had reasonably sized values. In principle, the kinetic constant can be evaluated too; in which case, the absolute values of the nucleation free energy would be available. In practice, such an estimation will be very difficult and is beyond this present study. The "semiempirical" method for the calculation of the rate and energy of heterogeneous nucleation on a unique particle can be applied to the data in Figure 6. The results of these calculations are presented in Table 1.

TABLE 1: Calculations of the Nucleation Rate, $J_c t_0$, and the Gibbs Energy, $\Delta G^*_{het}/kT$, from the Experimental Data of Condensation of the Octadecanol Vapor on Ag Nanoparticles at Different Supersaturation Values

	$R_0 = 1.400$ nm, $W(R_0) = 0.186$				
P, mPa	3.52	6.75	14.59	29.29	54.75
P_{cn}	0.102	0.151	0.167	0.166	0.162
$J_c t_0$	0.792	1.665	2.297	2.245	2.048
J_c at $t_0 = 0.3$ s	2.637	5.549	7.657	7.484	6.826
$\gamma = -\ln(J_c t_0/R_0^2)$	0.906	0.163	−0.159	−0.136	−0.044
$\Delta G^*_{het}/kT$ + const	1.906	1.163	0.841	0.864	0.956
	$R_0 = 1.67$ nm, $W(R_0) = 0.295$				
P_{cn}	0.148	0.209	0.223	0.240	0.244
$J_c t_0$	0.696	1.236	1.414	1.271	1.749
J_c at $t_0 = 0.3$ s	2.322	4.120	4.715	4.237	5.831
$\gamma = -\ln(J_c t_0/R_0^2)$	1.382	0.808	0.673	0.780	0.461
$\Delta G^*_{het}/kT$ + const	2.382	1.808	1.673	1.780	1.461
	$R_0 = 1.98$ nm, $W(R_0) = 0.296$				
P_{cn}	0.700	0.114	0.173	0.202	0.218
$J_c t_0$	0.270	0.486	0.878	1.147	1.331
J_c at $t_0 = 0.3$ s	0.899	1.621	2.927	3.824	4.437
$\gamma = -\ln(J_c t_0/R_0^2)$	2.672	2.088	1.496	1.229	1.080
$\Delta G^*_{het}/kT$ + const	3.672	3.088	2.496	2.229	2.080

Discussion

Rate and Energy of Nucleation. Figures 11 and 12 present empirical calculations of the energy and rate of nucleation condensation on single aerosol particles in accordance with eqs 23 and 24. The values presented are approximations since there are significant uncertainties in supersaturation and some of the other input parameters. The relative values should be reasonably correct, but the absolute values are much less certain.

As can be seen, the empirical dependence of the nucleation rate and Gibbs energy are nonmonotonic for the smaller values of particle size. Thus, the experimental data demonstrate double-barrier nucleation that had previously only been predicted theoretically. It can be concluded that the case of heterophilic

particles corresponds to these experimental data and thereby justifies the theoretical approach and resulting model. On this basis, the observed size spectrum transformations can be understood.

Qualitative Explanation of the Size Spectrum of Heterophilic CN. During the transformation of the distribution from unimodal to bimodal depending on the particle radius and the supersaturation, the energy of heterogeneous nucleation will be a nonmonotonic function of these variables. As seen above, cases were observed for heterophilic particles when the critical embryo overlaps an active site for small particles or at low saturations and when the embryo can be placed within an active site on larger particles or at higher supersaturations.

It follows from Fletcher's nucleation theory that, for homophilic particles, the energy and the rate of heterogeneous nucleation are smooth monotonic functions of the particle radius. Therefore, during vapor condensation on such particles, their ("dry") initial spectrum will only be "shifted" in the direction of larger sizes (Figure 5). However, for heterophilic particles, during the size spectrum evolution of an aerosol ensemble in supersaturated vapor, the theory predicts there will be a change from an initial monomodal size distribution of heterophilic particles into bimodal or even trimodal distributions as heterogeneous nucleation and growth proceed. The effects of the surface heterogeneity and double-barrier nucleation explain the observed size spectral transformations in the CNC experiments.

Additionally, it can be suggested that nucleation of vapor onto "active sites" of nanoparticles could provoke a specific "condensation jet" effect (CJE) resulting in an anisotropic impulse given to the particle by the condensing vapor molecules.[33] The hypothetic CJE seems to be much stronger than the Brownian motion of the particles. Thus, as a result of the CJE, nanoparticles acquire additional velocity, and thereby the efficiency of coagulation of heterophilic nanoparticles during heterogeneous condensation can be increased. Such a stimulated coagulation may be called the "condensation jet stimulated coagulation" (CJSC). The CJSC effect should also lead to the particle size spectrum transformation. It can be suggested that the third maxima in some of the condensation size spectra observed in the CNC are results of such effects. Theoretical estimations of the CJE and the CJSC effects will be performed and reported in future publications.

Summary

A working hypothesis has been examined that the surface heterophilicity of the CN nanoparticles influences their nucleation and condensation properties based on an advanced theory of the DBN effect. To link the experimental data on condensation activation of CN with their nucleation properties, a new "semiempirical" method was presented. This method permitted the estimation of the rate and free energy of heterogeneous nucleation on specific particles from the ensemble of condensational particle size distributions.

Summarizing the results, it can be concluded that the energy and rate of heterogeneous nucleation of polar liquids on heterophilic aerosol particles at a constant supersaturation depends on the particles size. For smaller particles, the rate is smaller (overlapping of the "site" by the critical embryo). For larger particles the rate is higher due to the role of increased numbers of "active sites". In some cases, DBN can occur that stops the nucleation. Therefore, depending on the particle size and supersaturation, heterophilic particles can have different "activation" behaviors.

We have also suggested that selective condensation on active sites of heterophilic particles could produce additional motion in those particles and initiate "condensation jet stimulated coagulation" (CJSC). CJSC could sufficiently increase the probability of coagulation that Brownian coagulation vanishes. The CJSC effect could also lead to a particle size spectrum transformation that would produce the third maxima observed in some experimental size distributions.

From this theoretical viewpoint, the evolution of the size spectrum of an aerosol ensemble in a supersaturated atmosphere of vapors can be expected to behave such that an initial monomodal size distribution of heterophilic particles can develop into a bimodal (or even trimodal) distribution. For homophilic particles, their initial size spectrum will only "shift" in the direction of larger sizes. The surface heterogeneity shown in this work does not depend on the nature of the theory used in the calculations, and classical nucleation theory that was applied in this research can be easily replaced with other approaches. In future studies, theoretical and experimental methods will need to be applied to provide a more quantitative analysis of the size spectrum distributions. We hope to investigate and present results on the complete problem, taking into account heterophilicity, roughness, and linear tension effects, as well as widening frames of classical nucleation theory in the future, after additional gathering of all needed experimental data.

Acknowledgment. This research was supported by the U.S. Environmental Protection Agency under Science to Achieve Results (STAR) Grant No. R826654 to Clarkson University. We would like to thank Dr. Michael Anisimov for the heat and mass transfer calculations to provide the estimates of the supersaturation.

References and Notes

(1) Harrison, R. M., Grieken, R. V., Eds. *Atmospheric Particles*; John Wiley & Sons: Chichester, 1998.
(2) Oberdoerster G. *Int. Arch. Occup. Environ. Health* **2001**, *74*, 1.
(3) Mavliev, R.; Hopke, P. K.; Wang, H.-C.; Lee, D.-W. *Aerosol Sci. Technol.* **2001**, *35*, 586.
(4) Mavliev, R.; Hopke, P. K.; Wang, H.-C.; Lee, D.-W. *J. Phys. Chem. B* **2004**, *108*, 4558.
(5) Lee, D. W.; Hopke, P. K.; Mavliev, R.; Wang, H. C. *J. Phys. Chem. B* **2003**, *107*, 13813.
(6) Köhler, H. *Trans. Faraday Soc.* **1936**, *2*, 1152.
(7) Meszaros, E. *Idojaras* **1969**, *73*, 1.
(8) Hänel, G. *Adv. Geophys.* **1976**, *19*, 73.
(9) Smorodin, V. Ye. In *Reports of the Weather Modification Department*; Central Aerologic Observatory: Moscow, 1985.
(10) Smorodin, V. Ye. In *Atmospheric Aerosols and Nucleation*; Fukuta, N., Wagner, P., Eds.; A Deepak Publ.: Hampton, VA, 1992; pp 295−300.
(11) Krastanov, L. *Idojaras* **1957**, *61*, 333.
(12) Fletcher, N. H. *Physics of Rainclouds*; Cambridge University Press: London, 1962.
(13) Smorodin, V. Ye. In *Circulation of Atmosphere and Moisture Transfer over the Central and East Europe. Abstracts of the International Symposium of Interdepartmental Commission at the USSR*, Moscow, 1983; pp 12−13.
(14) Smorodin, V. Ye.; Bazzaev, T. V. *Trudy Tsentralnoy Aerologitcheskoy Observatorii* (Russian) **1986**, 162−169.
(15) Almazov, L. A.; Smorodin, V. Ye. *Colloidal J. U.S.S.R.* **1990**, *52*, 275−280; *52*, 979−988.
(16) Mahata, P. C.; Alofs, D. J. *J. Atmos. Sci.* **1975**, *32*, 116.
(17) Hamill, P.; Turco, R. P.; Kiang C. S.; Toon, O. B.; Whitten, R. C. *J. Aerosol Sci.* **1982**, *13*, 561.
(18) Malm W. C. In *Organic Chemistry of the Atmosphere*; Hansen, L. D., Eatough, D. J., Eds.; CRC Press: Boca Raton, FL, 2000; p 284.
(19) Smorodin, V. Ye. *Rep. U.S.S.R. Acad. Sci. Ser. Phys. Atmos. Ocean* **1990**, *26* (8), 820.
(20) Smorodin, V. Ye. *J. Aerosol Sci.* **1990**, *21* (Suppl. 1), 249.
(21) Smorodin, V. Ye. *Atmos. Res.* **1994**, *31*, 199.
(22) Tovbin, M. V.; Golovchenko O. L.; Smorodin, V. Ye. *Ukr. Phys. J.* (Russian) **1978**, *24*, 415.

(23) Almazov, L. A.; Smorodin, V. Ye.; Tovbin, M. V. *Colloidal J. U.S.S.R.* **1980**, *42*, 171.
(24) Smorodin, V. Ye. *Langmuir* **1994**, *10*, 2250.
(25) Smorodin, V. Ye. *Soviet Phys. Dokl.* **1987**, *297*, 593.
(26) Lazarides, M.; Hov, Ø.; Eleftheridadis, K. *Atmos. Res.* **2000**, *55*, 103.
(27) Scherbakov, L. M. *Colloidal J. U.S.S.R.* **1952**, *14*, 379.
(28) Scherbakov, L. M. *Zh. Phizicheskoy Khim.* (Russian) ***1960***, *34*, 2120.
(29) Scheludko, A.; Toshev, B. V.; Platikanov, D. In *Modern Theory of Capillarity. Moscow, "Mir"* 1980; pp 274−299.
(30) Lazaridis, M. *J. Colloid Interface Sci.* **1994**, *162*, 431.
(31) Smorodin, V. Ye. *Phys. Chem. U.S.S.R.* **1988**, *302* (4−6), 910.
(32) Carte, A. E. *Proc. Phys. Soc.* **1959**, *73*, 324−327.
(33) Melikhov, I. V.; Simonov, E. F.; Vedernikov, A. A.; Berdonosov, S. S.; Bojevolnov, V. E. *Russian Chemical J.* (Russian) **1997**, *41*, 5.